

EUROPEAN ORGANIZATION FOR NUCLEAR RESEARCH
CERN — SL DIVISION

CERN SL-98-025 RF

The Quadrupole Resonator: Construction, RF System Field Calculations and First Applications

E. Chiaveri, E. Haebel, E. Mahner and J.-M. Tessier

Abstract

The quadrupole resonator allows measurement of the RF properties of superconducting (sc) films deposited on disk-shaped metallic substrates. We describe the construction of the apparatus, the brazing and electron-beam welding procedures, the arrangements for compensating mechanical tolerances of samples and for assuring reproducible sample illumination. We explain the special features of the RF system and give the results of field calculations with a 3D cavity code. Finally we present first measurements of Nb on Cu film samples and compare them with calibrations done with a bulk Nb sample.

*Presented at EPAC-98, 6th European Particle Accelerator Conference
Stockholm
22-26 June 1998*

Geneva, Switzerland
June, 1998

THE QUADRUPOLE RESONATOR: CONSTRUCTION, RF SYSTEM, FIELD CALCULATIONS AND FIRST APPLICATIONS.

E. Chiaveri, E. Haebel, E. Mahner, J.M. Tessier, CERN, Geneva, Switzerland

Abstract

The quadrupole resonator allows measurement of the RF properties of superconducting (sc) films deposited on disk-shaped metallic substrates. We describe the construction of the apparatus, the brazing and electron-beam welding procedures, the arrangements for compensating mechanical tolerances of samples and for assuring reproducible sample illumination. We explain the special features of the RF system and give the results of field calculations with a 3D cavity code. Finally we present first measurements of Nb on Cu film samples and compare them with calibrations done with a bulk Nb sample.

1 GENERAL DESCRIPTION

The 400 MHz quadrupole resonator is a screened, 4-wire transmission line circuit and is thus compact, compared to a cavity (Fig. 1). Resonance is established by placing short circuits on the line in two planes at a distance of $\lambda/2$. One of the shorts is the cylindrical screening enclosure's upper coverplate to which the Nb tubes of 16 mm \varnothing forming the wires are welded.

The other short is between pairs of these tubes and is realized by 10x10 mm square Nb tube sections, bent to form half rings of 20 mm radius. The resulting loop illuminates the front disk of the test cylinder ($\varnothing = 75$ mm) i.e. the sc film which had been deposited for RF testing.

Using stainless steel flanges with Conflat[®] seals the test cylinder is mounted into a tubular port of 2 mm bigger radius and equal length (80 mm) to make the sample surface flush with the lower coverplate of the enclosure, to which the port is welded.

Since the RF fields in the gap have quadrupole symmetry, they are at 400 MHz in cut-off and they decay with a rate of ≈ 1 dB/mm, i.e. the field strength at the flanges is negligible. This is the prerequisite to the use of a calorimetric method of RF dissipation measurement.

The test-cylinders for sc film tests have a composite front-disk made up of an outer Nb ring of 4 mm width (formed together with the cylinder's Nb side wall) and a central copper disc of 67 mm \varnothing electron beam welded to it. The deposited film covers the welding seam where substrate properties may not be well defined. This is not very important, as the field at the seam is only 10% of the full field at the loop.

The cylindrical screening enclosure ($\varnothing = 210$ mm, $L = 361$ mm) is composed of two niobium cans which are electron beam welded and vacuum brazed to the stainless steel flanges (DN 200) in the middle. Positioned at $\lambda/4$ from the upper cover plate the flanges are at a zero of the screening current and allow the apparatus to be opened for cleaning and inspection.

The coverplates themselves are flexible and special mechanical supports are provided to assure colinearity of the resonator rods with the system axis and to reproduce the 1 mm distance between loop and sample surface when samples are changed. This distance d is controlled by measuring at room temperature frequencies of different modes, and especially of the monopolar mode (currents on the 4 wires are in phase), whose frequency is most sensitive to changes of d .

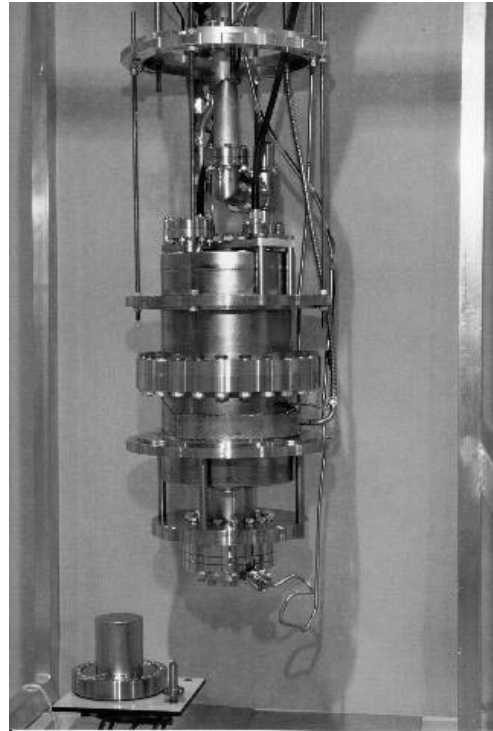


Figure 1 : The quadrupole resonator

2 RF SYSTEM DESCRIPTION

Coupling to the resonator is realized by two strongly over-coupled ($\beta \approx 100$) loops on the upper cover plate. Since sample dissipation is measured by calorimetry no determination of Q_0 is needed and it is of advantage to over-couple strongly. Loop calibration (Q_{ex} value) is readily obtained by the relation $Q_{ex} = 2 QL$. QL has

been measured both by the bandwidth and by the free decay method: $Q_L = 2.5 \cdot 10^6$. The comfortable bandwidth, which results from over-coupling, is also needed since the resonator is sensitive to external mechanical noise sources and to ponderomotive oscillations, especially for high RF fields. To avoid such mechanical oscillations, we have to operate at the resonance or on its safe side, where no oscillation occurs [1]. Measuring P_t allows the stored energy U to be determined ($\omega U = Q_{ex} P_t$) and therefore, via a cavity code, the fields at the sample's surface. The RF system around the resonator follows the classical Pound scheme. Samples of the incident and transmitted RF signals are processed to produce a dc control voltage proportional to their phase difference, and used to pull the generator frequency onto the cavity frequency.

3 FIELD CALCULATIONS

Although after calibration with a known test sample R_s can be determined without the exact knowledge of H [2], we attempted to relate stored energy and sample fields in using a 3D cavity code (MAFIA). It is difficult to find a mesh configuration fine enough to accurately resolve the fields between loop and sample without exceeding the maximally allowed number of mesh-points. Finally, at the main flange (at $\lambda/4$ from the upper coverplate), the resonator volume was split and a magnetic boundary put there. After calculating both parts separately with the same mesh precision and matching E-fields at the magnetic boundary the total stored energy could be obtained.

As in cavity work and in analogy to the notion of (R/Q) we now can express the relation between the maximal value of the magnetic sample field H_{max} and the stored energy U by a figure of merit with the dimension of a conductance per square meter :

$$K = \frac{H_{max}^2}{2\omega U} (AV^{-1}m^{-2})$$

For our resonator, K takes the value of 13.24. As a direct check of the H field calibration we intend to measure a tin sample. There reaching the critical field should have a marked effect on the dissipation.

Figure 2 and Figure 3 show the magnitude of the magnetic surface field on two perpendicular lines from the centre to the edge of the disk, the first passing under the centre of a half loop, the second in between the two half loops. The field reaches its maximum on the first line, under the loop and decreases steeply away from it. The ratio between the highest value below the loop and the highest value at the edge of the sample is about 15.

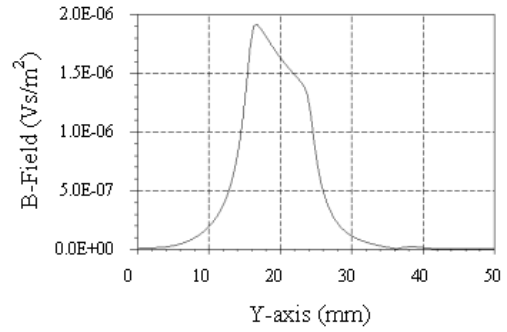


Figure 2 : Magnitude of the surface field on a line from the disk centre to its edge passing under the centre of a half loop

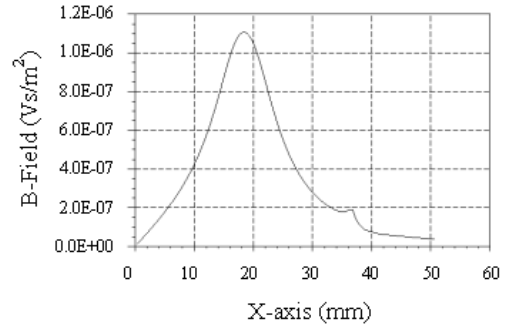


Figure 3 : Magnitude of the surface field on a line from the disk centre to its edge passing in between the two half loops

4 FIRST SC FILM MEASUREMENTS

In the companion paper a test cylinder from bulk niobium allowed the relation between surface resistance (R_s) and the power ratio P_{diss}/P_t to be determined. P_{diss} is the sample dissipation measured by calorimetry. Based on this calibration we now are presenting first measurements of sc films.

Since we are interested to preview the performance of such a film in a LEP cavity, we plot on the ordinate the ratio of the LEP geometry factor ($G_{LEP} = 232$) and the measured R_s , which results in an equivalent quality factor. On the abscissa, we plot an equivalent accelerating gradient (E_{equiv}), using the known ratio of the maximum magnetic field and the accelerating gradient of the LEP cavities ($H_{max}/E_{acc} = 31 \text{ Acm}^{-1}/\text{MVm}^{-1}$) and in equating the maximal surface field on the sample and in the cavity.

All measurements were done with a He bath pressure of 40 mbar, corresponding to a temperature of 2.11 K. Two different Nb/Cu Samples were tested. The first was coated at the equator of a LEP cavity mock up, i.e. sputtered with an incident angle of 90° , the second, in an iris near position, with an angle of 15° . To allow comparisons, we brought also the bulk Nb results in the same format (Fig. 4).

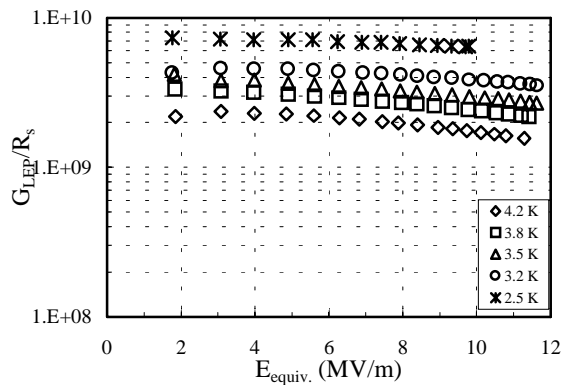


Figure 4 : Bulk Nb results

The first Nb/Cu sample (90° incidence) shows a very small H field dependence but a very low Q_0 even at the lowest temperatures (Fig. 5). Probably a surface defect masks the real sc properties of the coating. The second Nb/Cu sample (15° incidence) shows a strong H field dependence and a rather high surface resistance even at low temperature and field. This result corroborates the hypothesis made to explain the low Q_0 of sputtered low β cavities [3]. More tests have to be made to confirm this first result.

As a coarse test whether the bulk Nb R_s calibration was also valid for the Nb/Cu measurements, we have plotted the surface resistance at 3 MV/m of all three samples against $1/T$ (Fig. 7). At high temperatures (near T_C), where the BCS resistance dominates, the three curves merge as expected.

5 ACKNOWLEDGEMENTS

The authors want to thank all members of the SL/RF group who contributed to the realisation of this new instrument. Special thanks go to D. Moriaud for manufacturing high precision Nb parts, to E. Magnani and B. Thony for finding solutions to conflicting demands in mechanical construction and assembly, to F. Grabowski for cabling, to J.F. Malo for help with the RF system, and to A. Insomby and H. Preis for supervising the clean room, vacuum and cryogenic aspects of the experimental set-up. S. Calatroni prepared the first sputtered Nb/Cu samples.

REFERENCES

- [1] D. Boussard, P. Brown, J. Tuckmantel, "Electroacoustic instabilities in the LEP2 sc cavities", CERN-SL-95-81-RF.
- [2] E. Haebel, E. Brigant, E. Mahner, "The quadrupole resonator, design considerations and layout of a new instrument for the RF characterisation of superconducting surface samples", EPAC 98.

- [3] C. Benvenuti, D. Boussard, S. Calatroni, E. Chiaveri, J. Tuckmantel, "Production and test of 352 MHz niobium-sputtered reduced- β cavities", CERN-SL-97-063-RF.

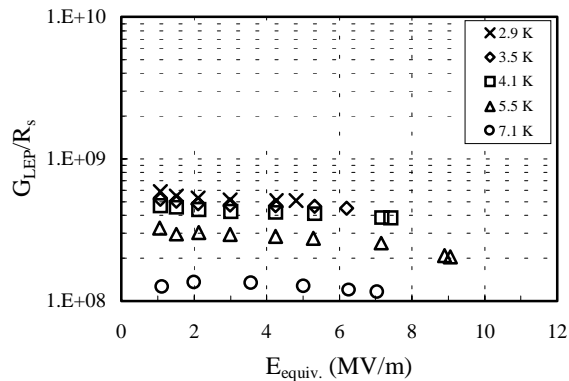


Figure 5 : Nb/Cu sample (90° incidence)

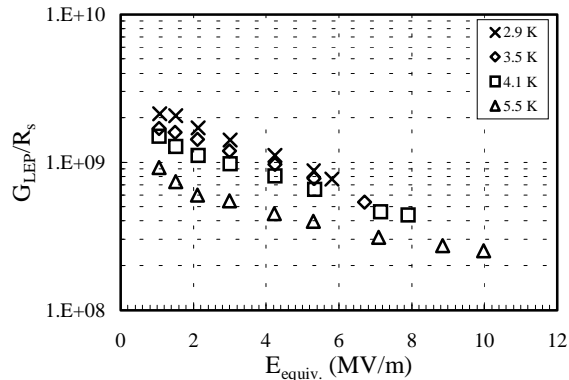
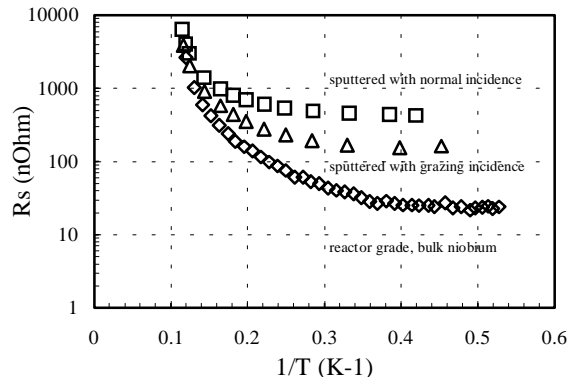


Figure 6 : Nb/Cu sample (15° incidence)

Figure 7 : R_s versus $1/T$ for the 3 samples.